

Rocket Measurement of Ozone Density Distribution in the Equatorial Stratosphere & Mesosphere

Y V SOMAYAJULU & K S ZALPURI

Radio Science Division, National Physical Laboratory, New Delhi 110012

and

S SAMPATH

Atmospheric Science Division, Centre for Earth Science Studies, Trivandrum 695010

Received 24 July 1981

The ozone density distribution in the middle atmosphere measured from a Centaure II rocket flight by using the absorption photometry technique in the UV range at 2550 Å is presented. The ozone profile obtained from the data in the altitude range 45-95 km shows a good agreement with the results obtained by other workers in the region 50-70 km. The important features of the observed profile are the presence of a valley in the ozone distribution around 78 km and a secondary peak around 90 km. These are in qualitative agreement with other measurements for large solar zenith angles although the magnitude of the values at the peak is unexpectedly large.

1. Introduction

Ozone is an important minor neutral constituent of the middle atmosphere and provides a heat source by absorbing the solar UV radiations in the Hartley and Huggins bands. Consequently it shields the biological activity on the earth's surface from the harmful effects of these radiations. It is also important for studying the chemistry of the neutral and charged species in the middle atmosphere. Recently considerable interest in ozone significantly and thereby cause health by the suggestion that the nitric oxide injected by supersonic aircrafts could deplete the stratospheric ozone significantly and thereby causing health hazards. More recently other suggestions have been made that use of nitrogen fertilizers, aerosols, etc. could also seriously affect the ozone distribution. It is recognized that the NO_x , HO_x and ClO_x compounds can catalytically destroy ozone, if injected in sufficient quantities. Recently considerable amount of efforts have been put in to measure its concentration with the help of rockets and satellites in midlatitudes¹⁻⁵. However, at low latitudes, only a few measurements exist, and hardly any at large solar zenith angles at which ozone variability is expected to be maximum. In this paper the ozone density distributions in the upper stratosphere and mesosphere measured from a rocket flight conducted from Thumba, India, at the geomagnetic equator, using absorption photometry technique, are presented.

2. Description of the Experiment

A Centaure II rocket was launched from Thumba (8°34'N, 76°52'E), India, on 18 Feb. 1980 at the

geomagnetic equator as part of the Solar Eclipse Campaign of 16 Feb. 1980 at 0720 hrs IST (solar zenith angle = 82°). It carried an instrumented payload for the measurement of ozone concentration in the stratosphere and mesosphere. The technique employed is based on absorption photometry in the Hartley continuum of solar UV radiation at 2550 Å which is mainly absorbed by ozone in the atmosphere. This technique of absorption photometry also allows us to compare directly our results with those derived from remote sensing from satellites by means of UV spectrometers using the solar and stellar occultation techniques⁵.

The photometer used for this flight consisted of a combination of solar blind Cs-Te phototube and an interference filter with half-width of about 150 Å and maximum transmittance of 14% at 2550 Å. The advantage of choosing this particular wavelength in Hartley band is that the absorption cross-section of ozone in the vicinity of this wavelength is practically constant and thus derivation of ozone concentration from the measured intensity is simplified adopting constant absorption cross-section value. The interference filter and the phototube were calibrated prior to the flight, and the filter transmittance and quantum efficiency of the phototube obtained as a function of wavelength are shown in the inset in Fig. 1.

The output of the photometer was connected to a detector circuit having a linear response. An inflight calibration for the detector circuit was also provided every 90 sec to check its in-flight performance. A solar aspect sensor was also included in the same payload to provide data on the solar aspect angle, i.e. angle

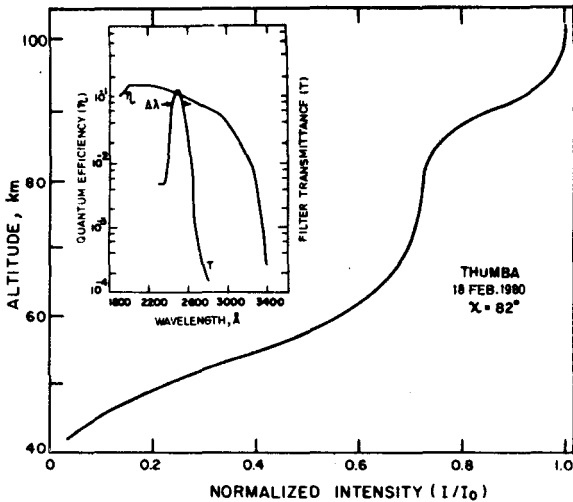


Fig. 1—Normalized intensity profile as a function of altitude (The spectral response of the interference filter and phototube is shown in the inset.)

between the longitudinal axis of the rocket and sensor-sun line. Using the data from the aspect sensor, the output of the photometer was corrected for the off-axis response due to solar aspect.

3. Theory of the Technique

Assuming that the monochromatic solar irradiance obeys Beer's law and taking into account the finite spectral width of the photometer, the normalized irradiance at any altitude z is given by

$$(I_z/I_0) = \frac{\int F(\lambda)T(\lambda)\eta(\lambda)\exp[-\sigma(\lambda)N(O_3, z)X]d\lambda}{\int F(\lambda)T(\lambda)\eta(\lambda)d\lambda} \dots(1)$$

where

I_z and I_0 Signal intensities at the altitude z and top of the atmosphere, respectively

$T(\lambda)$ Transmittance of the filter at wavelength λ

$\eta(\lambda)$ Quantum efficiency of the phototube at wavelength

$F(\lambda)$ Unattenuated solar irradiance value at the top of the atmosphere at wavelength λ

$\sigma(\lambda)$ Absorption cross-section of ozone at wavelength λ

X Optical depth factor equals to the chapman function $ch(X, H)$, for this case with constant scale height

$N(O_3, z)$ Column density of ozone at altitude z

To obtain the value of $N(O_3, z)$ from Eq. (1), numerical simulation method was used. For this, the attenuation of the solar flux given by normalized irradiance is calculated for different values of $N(O_3, z)$ in the range $10^{12} \leq N(O_3, z) \leq 10^{22}$ with an interval of $N(O_3, z)/10$. Using these calculated values, the observed normalized irradiance is converted into ozone column density.

In this study for the solar irradiance, values as suggested by Broadfoot⁶ as 10 \AA average in the wavelength region $2100\text{-}3200 \text{ \AA}$ are used. For absorption cross-section for ozone, values suggested by Inn and Tanaka⁷ are adopted. Finally from the ozone column density values the number density of ozone was determined by using the following relation.

$$N(O_3, z) = \int n(O_3, z) dz \dots(2)$$

4. Results and Discussion

Using the solar aspect data the telemetry data from this experiment was first corrected for the off-axis response of the photometer due to finite solar aspect angle. The altitude versus detector output data is then fitted with a smooth curve. The normalized intensity profile thus derived is shown in Fig. 1.

By using the method described in Sec. 3, the altitude-current profile was inverted to derive the ozone number density distribution as a function of altitude, and the profile thus obtained is shown in Fig. 2. The total error, including the systematic error, is estimated to be about $\pm 8.5\%$ between 45 and 70 km. At higher altitudes the accuracy deteriorates owing to the difficulty in measuring the small absorption values and due to uncertainties in heights due to lack of knowledge of vehicle precession. The random errors in this region dominate the total measurement errors as estimated from the jitter in the data. It is estimated that the maximum total error in the derived density values is about $\pm 45\%$ above 70 km.

In Fig. 2 are also shown the experimental profiles derived from other rocket experiments using UV spectroscopy⁸, satellite occultation of solar and stellar UV radiation^{5,9} and the mid-latitude empirical model of Krueger and Minzner¹ based on an extensive series of rocket experiments. In addition theoretical models of Shimazaki and Laird¹⁰ and Ogawa and Shimazaki¹¹ are also shown.

It is seen that the ozone density profile obtained from the present experiment below 75 km is in qualitative agreement with other experimental profiles; quantitatively, below 60 km, the observed values are lower than those observed by other workers by a factor of 3 at 50 km and this difference decreases with the increase of altitude. However, compared to the values derived⁵ from satellite UV occultation, the values are somewhat higher, for example, by a factor of 2.5 at 50 km. A qualitative feature shown, in consistency with others, is the presence of two approximately exponential slopes—one below 60 km and the other above.

The other features in the observed ozone density distribution are the presence of a valley in the 76-82 km region and a mesospheric secondary peak at 90 km. The mesospheric secondary peaks had been reported from

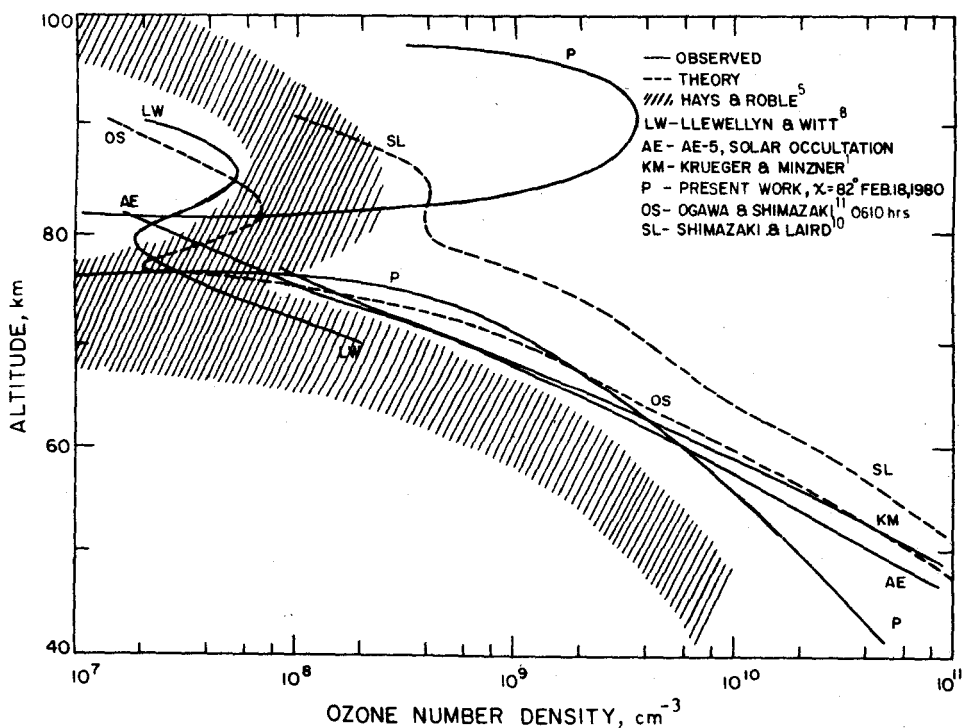


Fig. 2—Ozone number density profile as a function of altitude (For comparison the other experimental and theoretical profiles are also shown.)

nighttime measurements⁵ and from daytime measurement¹² for solar zenith angle of 88° . However, quantitatively, the magnitude of the peak density is higher by an order of magnitude. The sensor was mounted at an angle of 95° to the spin axis of the rocket so as to enable it to look towards the sun. The field-of-view of the sensor was about 50° . Therefore, it was possible that the sensor during flight received contribution from diffusely reflected or backscattered radiations in this altitude region which could probably cause the overestimation of ozone density. While the values are much higher than ever reported (considering all the sources of error), the existence of a secondary mesospheric sunrise peak is considered to be genuine. Considering the chemistry of ozone, it is mainly produced by the three body reaction as follows.



Since the neutral density values as given by CIRA¹³ models in the equatorial region are higher by about 10%, this by itself can contribute a 20% difference in the ozone production between mid- and equatorial latitudes. Atomic oxygen is also expected to vary with latitude¹⁴. Even taking into account such possible latitudinal variation, the observed values seem to be rather too high to be accounted for with currently existing theoretical models. The presence of the valley around 78 km is probably due to the fact that removal of ozone by photodissociation begins at this time while its production by reaction (3) is not appreciable because of

the low atomic oxygen concentration. In addition to photodissociation, the loss of ozone is partly due to its reaction with atomic hydrogen. Ogawa and Shimazaki¹¹ have shown that both atomic oxygen and atomic hydrogen decrease at night but the rate of decrease below 85 km depends upon the supply of these species from altitudes above by eddy diffusion, and the ozone valley around 78 km can be attributed to the larger ratio of decrease for atomic oxygen than for atomic hydrogen. Theoretical studies have also reproduced the mesospheric maximum in ozone distribution^{10,11,15}. These studies have demonstrated that the distinction and magnitude of this feature depend on the values of eddy diffusion coefficient and for large values of this coefficient, it almost disappears. However, to resolve the discrepancy about the higher values of ozone concentration around the mesospheric peak more measurements are to be carried out.

It was also found that taking a constant value ($1.3 \times 10^{17} \text{ cm}^2$) of absorption cross-section as suggested by Inn and Tanaka⁷, the difference in the derived values becomes less than 5%.

5. Conclusions

(i) The measured ozone profile below 70 km shows good agreement with other experimental and theoretical profiles, although below 50 km the values tend to be significantly low.

(ii) The presence of a valley in the ozone distribution around 78 km and a secondary peak in the mesosphere

around 90 km is observed. This is in qualitative agreement with other measurements for large solar zenith angles although the magnitude of values at the peak is unexpectedly large.

References

- 1 Krueger A J & Minzner R A, *J Geophys Res (USA)*, **81** (1976) 4477.
- 2 Nagata T, Tohmatsu T & Ogawa T, *Space Res (France)*, **11** (1971) 849.
- 3 Watanabe T, Zalpuri K S & Ogawa T, *Measurement of mesospheric ozone by S-310-6 rocket experiments*, Paper presented at the Symposium on Space Science Observations held in Tokyo, Japan, in June 1979.
- 4 Riegler G R, Drake J F, Liu S C & Cicerone R J, *J Geophys Res (USA)*, **81** (1976) 4997.
- 5 Hays P B & Roble R G, *Planet & Space Sci (GB)*, **21** (1973) 273.
- 6 Broadfoot A L, *Astrophys J (USA)*, **173** (1972) 681.
- 7 Inn E C Y & Tanaka Y, *J Opt Soc Am (USA)*, **43** (1953) 870.
- 8 Llewellyn E J & Witt G, *Planet & Space Sci (GB)*, **25** (1977) 165.
- 9 Guenther B, Dasgupta R & Heath D F, *Geophys Res Lett (USA)*, **4** (1977) 434.
- 10 Shimazaki T & Laird A R, *Radio Sci (USA)*, **7** (1972) 23.
- 11 Ogawa T & Shimazaki T, *J Geophys Res (USA)*, **80** (1975) 3945.
- 12 Weeks L H, Good R E, Randhawa J S & Trinks H, *J Geophys Res (USA)*, **83** (1978) 978.
- 13 CIRA, *COSPAR International Reference Atmosphere*, 1972.
- 14 Donahue T M, Guenther B & Thomas R J, *J Geophys Res (USA)*, **78** (1973) 6662.
- 15 Thomas L & Bowman M R, *J Atmos & Terr Phys (GB)*, **34** (1972) 1843.